Error Factors in SAR Wind Retrieval for Inshore Areas

Takeyama, Yuko; Ohsawa, Teruo; Kozai, Katsutoshi; Hasager, Charlotte Bay; Badger, Merete

Published in:
Proceedings (online)

Publication date:
2009

Document Version
Publisher's PDF, also known as Version of record

ERROR FACTORS IN SAR WIND RETRIEVAL FOR INSHORE AREAS

Yuko Takeyama [1)], Teruo Ohsawa [2)], Katsutoshi Kozai [2)], Charlotte Hasager [3)], Merete Badger [3)]
1) National Institute of Advanced Industrial Science and Technology (AIST)
Central 2, Umezono1-1-1, Tsukuba, Ibaraki, 305-8568, JAPAN
E-mail: takeyama.yuko@aist.go.jp Tel: +81-29-862-6723 Fax: +81-29-862-6610
2) Kobe University Graduate School of Maritime Sciences
3) Risoe National Laboratory for Sustainable Energy, Technical University of Denmark

Summary

In this paper, accuracy of Synthetic Aperture Radar (SAR)-derived wind speeds and its error factors are discussed by using 61 ENVISAT/ASAR images covering two inshore areas, Hiratsuka and Shirahama, in Japan. As a first step, effects of the pixel averaging size on the accuracy of retrieved wind speed are examined. The results show that the highest accuracy is obtained when 300m-averaging is applied for Hiratsuka (RMSE = 2.30 m/s) and 200m-averaging is applied for Shirahama (RMSE = 1.93 m/s). These results indicate that SAR-retrieved wind speeds in the inshore areas in Japan are less accurate than those reported in open oceans (approx. RMSE = 1 to 2 m/s). The errors can be caused by some phenomena particular to an inshore area. Thus, in order to evaluate the effect of fetch, the errors of SAR wind speeds are examined in terms of wind direction, distinguishing winds from land and sea sectors. As a result, the effect of fetch on the error of SAR-derived wind speed could not be clearly detected in this study. On the other hand, it is shown that SAR wind speeds depends on atmospheric stability and tend to be overestimated under the unstable atmospheric condition.

1. Introduction

SAR observing the Earth with high spatial resolution recurrently is expected for making of offshore wind resource map. SAR can retrieve sea surface wind speeds using a Geophysical Model Function (GMF), which is an empirical model to convert from intensity of backscattered microwaves to wind speed. Vachon *et al.* (1996) reported that the Root-Mean-Squared Error (RMSE) of SAR wind speeds is approximately 1.5 m/s using the GMF and other studies also reported that RMSE of SAR wind speeds usually is 1 to 2 m/s in open oceans. However it is not well known whether the GMF and the method of SAR wind speed retrieval can be applied with the same accuracy for inshore areas in Japan, which is characterized by complex terrains. Thus, this paper validates the SAR wind speeds retrieved in the inshore area in Japan.

It is conceivable that most errors of SAR wind speeds are caused by reliability of Normalized Radar Cross Section (NRCS), effect of speckle noise, uncertainty of wind direction and effects of oceanographic and atmospheric phenomena. Accuracy of NRCS depends on qualities of a sensor and calibration coefficients. The speckle noise is caused by scattering of coherent electromagnetic waves by rough surface (Goldfinger *et al*., 1982) and the effect of this noise can be down to below 0.2 dB for NRCS by degrading grid cell to 2 km × 2 km (Horstmann *et al*., 2000). However, few

kilometers or several tens of kilometers pixel-averaging can be applied in the open ocean, while few hundred meters may be a limit for the pixel-averaging in the inshore area because of short fetch. Therefore, it is necessary to detect the most suitable pixel-averaging sizes in the inshore area in consideration of the effect of the speckle noise. In this paper, we at first clarify relation between accuracies of SAR wind speeds and pixel-averaging sizes. And then, by using the most accurate SAR wind speed, other error factors caused by oceanographic and atmospheric phenomena peculiar to the inshore area are discussed.

2. Data and Methods

2.1 In situ Observation Data

For validating the SAR-retrieved wind speed, this study uses in situ observation of sea surface wind speed and direction from two offshore observation towers. One is the Hiratsuka observation tower (35°18′20″N, 139°20′45″E) operated by Institute of Industrial Science, the University of Tokyo (IIS) (Fig. 1). The other is the Shirahama observation tower (35°42′32″N, 135°19′58″E) operated by Disaster Prevention Research Institute (DPRI), Kyoto University (Fig. 1). The size of the two towers is roughly the same; the height is 23 m and the maximum diameter is less than 10 m. Hourly 10min-averaged wind speed and direction are measured at 23 m height above the Mean Sea Level (MSL) with a propeller anemometer at the both towers. These measured wind directions are used as input values to the GMF and wind speeds are used for accuracy validation of SAR-retrieved wind speed. Other oceanographic and atmospheric data, measured in both towers (Tables 1 and 2) are used for height correction of wind speed and calculation of atmospheric stability.

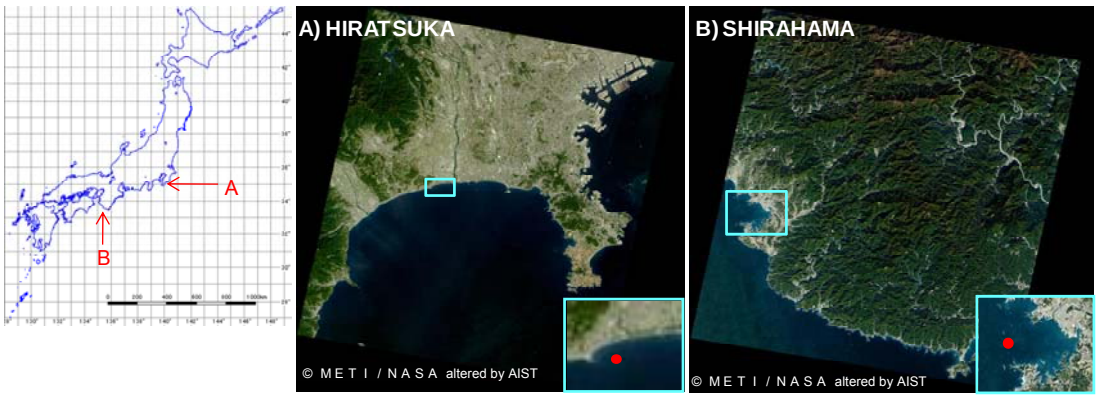

Fig.1 Geographical locations of the Hiratsuka (A) and Shirahama (B) stations (filled red circles).

Table 1 Observed elements at Hiratsuka station.

Observation Term	Observation Hight (reference MSL)	Remark
Air temperture	above 20m	Resistance temperature sensor
Sea temperture	below 3m	Resistance temperature sensor
Wind speed, Wind direction	above 23m	Propeller anemometer
Current speed, Current direction	below 7m	Geomagnetic electro kinetograph

Table 2 Observed elements at Shirahama station.

Observation Term	Observation Hight (reference MSL)	Remark
Air temperture	above 15m	Resistance temperature sensor
Sea temperture	below 5m	Resistance temperature sensor
Wind speed, Wind direction	above 23m	Propeller anemometer

2.2 ENVISAT/ASAR image and Geophysical Model Function (GMF)

ENVISAT was launched on March 1, 2002. Advanced Synthetic Aperture Radar (ASAR) onboard ENVISAT has been operating at C-band with the HH and VV polarizations. 61 ASAR Precision Mode images (Hiratsuka; 23 images and Shirahama; 38 images) are used in this study. Sea surface wind speed is generally calculated from a SAR image using a GMF, which relates the Normalized Radar Cross Section (NRCS) with wind speed, relative wind direction, and radar incidence angle. The C-band GMF called CMOD4 （eq.(1)）(Stoffelen *et al*, 1997) is used for wind speed retrieval in this study.

$$\sigma_{vv}^{0} = b_0\left(1.0 + b_1\cos\varphi + b_3\tanh\left(b_2\right)\cos\left(2\varphi\right)\right)^{1.6} \quad \cdots (1)$$

where σ^0_{vv} is NRCS observed by VV polarized microwaves, b0,b1 and b2 are coefficients depending on wind speed and radar incidence angle, φ is the relative angle defined as the radar-looking direction minus the wind direction. For HH polarized ASAR images, the Mouche *et al*. (2005)'s equation (eq. (2)) is used to compensate for the lower radar backscatter coefficient at HH polarization.

$$\sigma_{vv}^{0} / \sigma_{hh}^{0} = C_0\left(\theta\right) + C_1\left(\theta\right) + \cos\varphi + C_2\left(\theta\right)\cos 2\varphi \quad \cdots (2)$$

2.3 Height Correction of Wind Speed

Height correction of wind speed is necessary to compare observed wind speeds at 23 m above the MSL with SAR wind speeds at 10 m. In order to estimate 10 m wind speeds from 23 m observed wind speeds, we use the following vertical wind profile with the universal function Ψ(ζ) obtained from the Monin-Obukhov similarity theory,

$$U_z = \frac{u_*}{\kappa}\left(\ln\left(\frac{z}{z_0}\right) + \Psi(\xi)\right) \quad \cdots (3)$$

where U_z wind speed at z(m) height, u_* is friction velocity and z_0 is aerodynamic roughness length. The relation between z_0 and u_* is obtained from the Charnock's (1955) roughness length model as follows,

$$z_0 = z_{ch} \cdot u_*^2 / g \qquad (z_{ch} = 0.0185) \quad \cdots (4)$$

where z_{ch} is Charnock coefficient, which is taken from Wu (1980) and g is gravitational acceleration. The universal function Ψ(ζ) is defined as follow.

$$\begin{aligned} \Psi(\xi) &= 2\ln\left[(1+\phi)/2\right] - 2\tan^{-1}\phi + \pi/2 \qquad (\xi < 0) \\ \Psi(\xi) &= -\beta\xi \qquad (\xi > 0) \end{aligned} \quad \cdots (5)$$

where $\Phi=(1 - 16\zeta)^{1/4}$ and β=5. The non-dimensional stability parameter ζ= z/L is calculated as a function of the bulk Richardson number Rib, using the following formulation,

$$\begin{aligned} \xi &= 10 \cdot Rib\left(1 + Rib/-4.5\right)^{-1} \qquad (Rib < 0) \\ \xi &= 10 \cdot Rib\left(1 - 5Rib\right)^{-1} \qquad (Rib > 0) \end{aligned} \quad \cdots (6)$$

where $Rib = \frac{g}{\theta_{ave}} \frac{(\Delta\theta/\Delta z)}{(\Delta u/\Delta z)^2}$, Θ is potential temperature, Θ_{ave} is averaged potential temperature. z_0 and u_* can be solved simultaneously from equations (3) and (4). Then the ratio U_{10} / U_{23} can be estimated.

$$\frac{U_{10}}{U_{23}} = \frac{\ln\left(\frac{10}{Z_0} - \Psi\left(\frac{10}{L}\right)\right)}{\ln\left(\frac{23}{Z_{23}} - \Psi\left(\frac{23}{L}\right)\right)} \quad \cdots (7)$$

2.4 Method of Validation

Gash (1986) suggested the theory of footprint for winds over land, and then Semedman *et al*. (1999) adopt the theory to the ocean wind speed. According to this theory, wind speed is defined as weighted mean wind speed for the ellipsoidal upwind area. In the theory, the length scale is over few kilometers. However the shortest fetches are 1 km and 2 km in the Hiratsuka and Shirahama areas, respectively. If the theory is adopted for Hiratsuka or Shirahama, averaged wind speeds can include the effects from pixels including land. Thus, this paper examines the accuracy of SAR wind speeds when small averaging area sizes are adopted. This paper takes an average of wind speeds over the area with a diameter which is changed from 50 m to 1000 m. The Cressman scheme (Cressman, 1959) (eq. (8)) is used as the averaging method.

$$W_{i,j} = [\ (R^2 - d_{i,j}) \ / \ (R^2 + d_{i,j})\ ] \quad \cdots (8)$$

where R is a influence radius, which is a half of the averaging diameter, and d*ij* is distance from pixel locations to the each observation tower. Hereafter, “X m-averaging” means that the diameter of an influence circle for average is X m.

3. Relation between diameter of pixel averaging and accuracy

3.1 In case including the observation tower

Fig. 2 shows results of SAR wind speed retrieval when averaging area sizes are changed. Four statistical values (averaged wind speed, RMSE, bias and correlation coefficient) are found to be greatly changed in the range from 50 m to 200 m of averaging diameters for both sites, mainly due to the effect of strong backscatter from the observation tower itself. It is shown that the effect of strong backscatter caused by the observation tower itself is mostly disappeared in the range of more than 200-m averaging. In Fig. 2 (upper), 300m-averaging have the highest accuracy at Hiratsuka, and the RMSE, bias and correlation coefficient are 2.30 m/s, -0.59m/s and 0.76, respectively. Fig. 3 (left) shows scatterplot of 300m-averaging SAR wind speeds and measured wind speeds at Hiratsuka. SAR wind speeds are underestimated at Hiratsuka. Especially, the tendency of underestimation is remarkable when observed wind speeds are between 5 and 12 m/s. On the other hand, 200m-averaging has the highest accuracy at Shirahama (Fig. 2 (lower)), and the RMSE, bias and correlation coefficient are 1.93 m/s, - 0.71m/s and 0.74, respectively. The tendency of underestimation between 5 and 12 m/s seen at Hiratsuka is also found at Shirahama (Fig. 3 (right)). RMSE of SAR wind speeds are usually 1 to 2 m/s in open oceans as noted in Section 1. According to the results of comparison of RMSE values, it is found that the accuracies of SAR wind speeds in the inshore areas are lower than those in open oceans.

3.2 In case excluding the observation tower

In order to remove the effect of the observation tower, the center of an averaging area is moved toward offshore. The center is moved 500 m southeastward for Hiratsuka and 500m westward for Shirahama. Fig. 4 shows the four statistic values (same as Subsection 3.1) of SAR wind speeds when averaging areas are changed. 100m-averaging has the highest accuracy with RMSE of 2.21 m/s at Hiratsuka (Fig. 4 (upper)). It is shown that a smaller averaging area is more suitable for the SAR wind retrieval for Hiratsuka, compared to the case including the observation tower, in which the 300m-averaging has the highest accuracy. On the other hand, 1000m-averaging has the highest accuracy with RMSE of 2.02 m/s at Shirahama. It is shown that a larger averaging area is more suitable in this case than in the case including the observation tower.

In order to clarify the reason why the suitable averaging area is different between Hiratsuka and Shirahama, Fig. 5 shows magnified images of wind speed distribution around Hiratsuka (left) and Shirahama (right). The rectangle size of both image is roughly 2 km × 2 km. Measured wind speeds are 5.1 m/s (August 1, 2008) and 5.3 m/s (December 8, 2007),

respectively. The SAR-retrieved wind speed at Shirahama is higher than that at Hiratsuka, but both measured wind speeds are almost the same. This overestimation at Shirahama is due to the speckle noise, which can be clearly seen in Fig. 5 (right). Within the 61 images used in this study, the number of images including remarkable speckle noises is more for Shirahama than for Hiratsuka. Consequently, it can be said that in case with small effects of speckle noises, pixel averaging for a smaller area leads to more accurate wind retrieval, while a larger-area averaging is more effective for images with large effects of speckle noises.

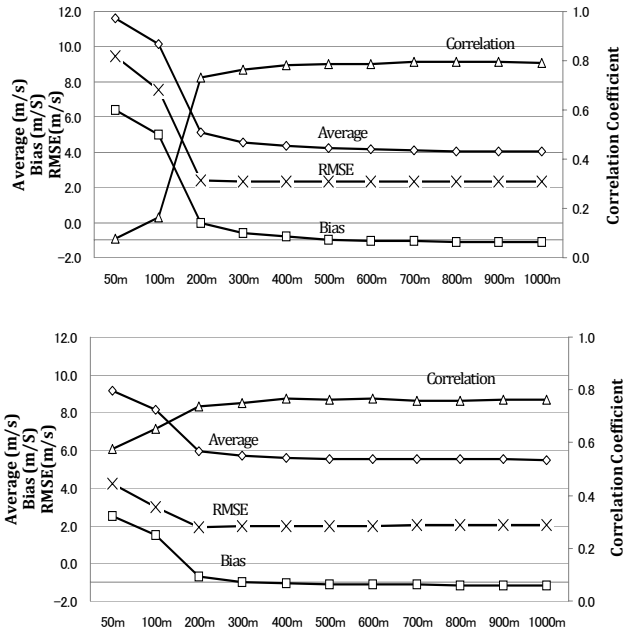

Fig. 2 Correlation coefficient, average (m/s), bias (m/s) and RMSE (m/s) of the wind speeds retrieved from 61 ASAR images and in-situ wind directions at Hiratsuka (upper) and Shirahama (lower). These statistical values are expressed as a function of diameter of pixel averaging.

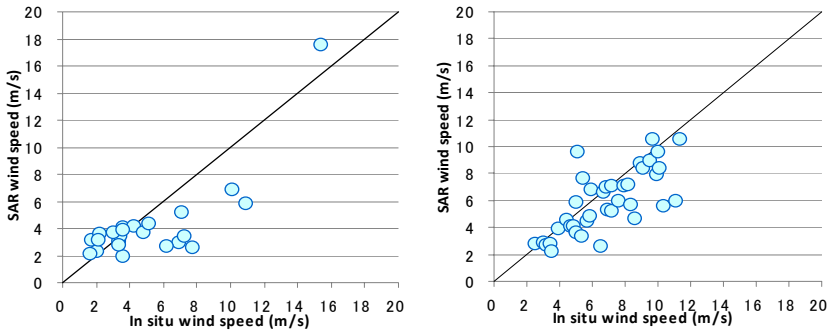

Fig. 3 Relation between in situ wind speed and SAR wind speed using 300m-averaging and 200m-averaging at Hiratsuka (left) and Shirahama (right), respectively.

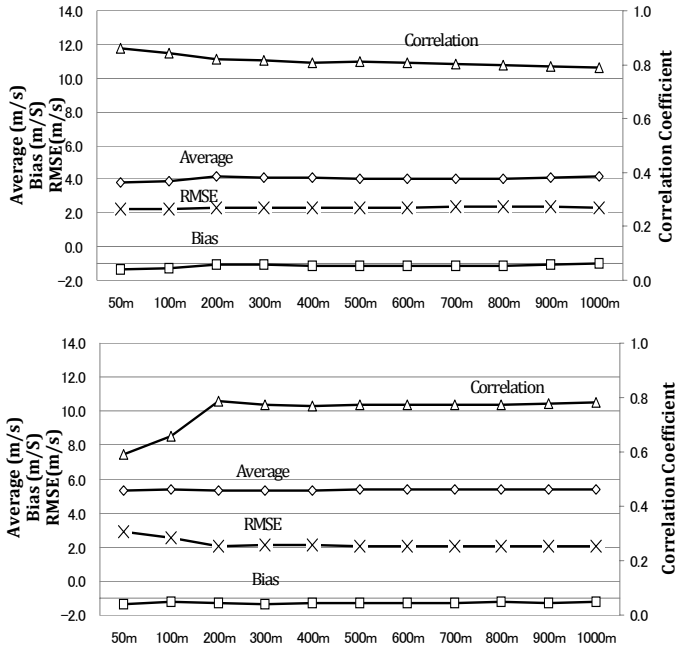

Fig. 4 Correlation coefficient, average (m/s), bias (m/s) and RMSE (m/s) of the wind speeds retrieved from 61 ASAR images and in-situ wind directions at Hiratsuka (upper) and Shirahama (lower). The center of an averaging area is moved 500 m from tower toward offshore.

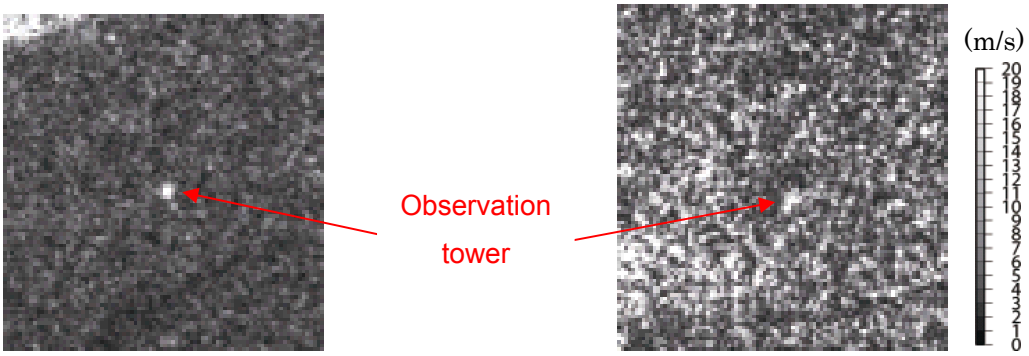

Fig. 5 Wind speed distribution around Hiratsuka (left) and Shirahama (right) towers. Measured wind speeds are 5.1 m/s (August 1, 2008) and 5.3 m/s (December 8, 2007), respectively. The both rectangle sizes of images are roughly 2 km ×2 km.

4. Effect of fetch

It is easy to imagine that fetch affects SAR wind speeds because sea surface wave cannot be fully developed in case with a short fetch in the inshore area when wind blows from land. However the relationship between the error of SAR wind speed and the fetch is not well known. Fig. 6 shows relation between wind directions and relative errors (%) of SAR wind speeds at Hiratsuka (Fig. 6 (upper)) and Shirahama (Fig. 6 (lower)). The relative error means the difference between retrieved

and measured wind speeds divided by measured wind speed. At Hiratsuka, north and south winds correspond to the winds from land and sea, respectively. In Fig. 6 (upper), it seems that relative errors of SAR wind speeds do not depend on the fetch. On the other hand, at Shirahama, westerly winds blow from the sea and northerly, easterly and southerly wind come from the land. Fig. 6 (lower) shows that SAR wind speeds of easterly and southerly winds (wind direction from 45° to 210°) are underestimated. For the westerly and northerly winds, both underestimation and overestimation can be seen. Therefore, it is also unclear from Fig. 6 (lower) that wind speed depends on fetch.

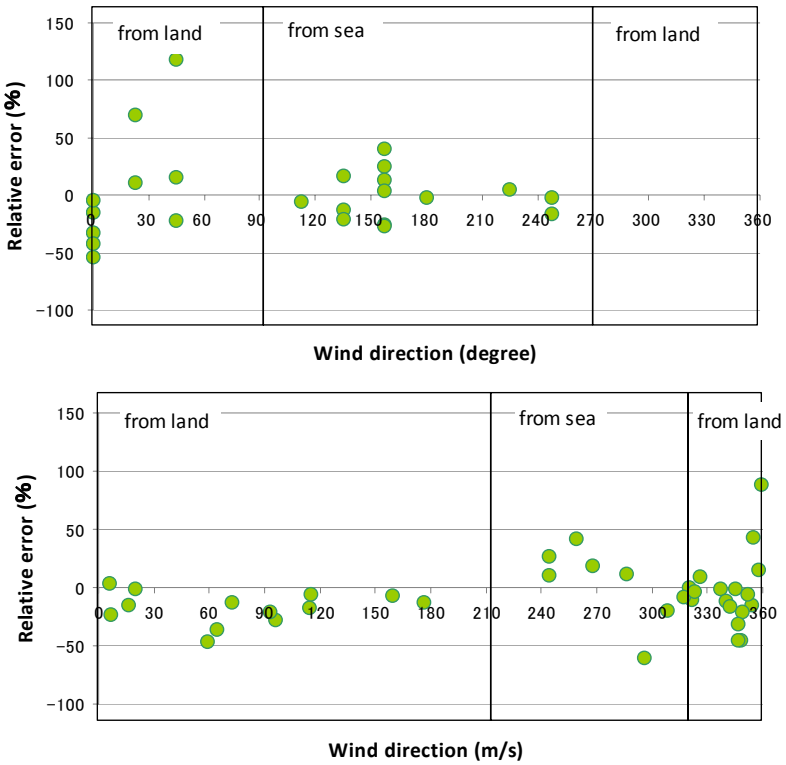

Fig.6 Relation between wind directions and relative errors (%) of SAR wind speeds for Hiratsuka (300m-averaging; upper) and Shirahama (200m-averagingl; lower) , respectively.

5. Atmospheric stability

Atmospheric stratification is easy to be unstable in the inshore area around Japan, because of cooler wind blowing from land and high sea surface temperature caused by the Kuroshio flowing on the Pacific side of the Japanese archipelago. Liu *et al*. (1996) reported that atmospheric stability affects SAR and scatterometer wind speed retrieval at low wind speed, and suggested that "Equivalent Neutral Wind", which is the wind speed expected under the assumption of neutral atmospheric stratification, has to be adopted for microwave wind speed sensing. Relation between bulk Richardson number and relative error of SAR wind speeds is shown in Fig. 7. It is noted that

Fig. 7 shows only the cases with wind speed of less than 6 m/s in order to see the effect of atmospheric stability more clearly. As the result, it is found that the SAR wind speed tends to be overestimated in unstable conditions (Rib<0) for both Hiratsuka and Shirahama.

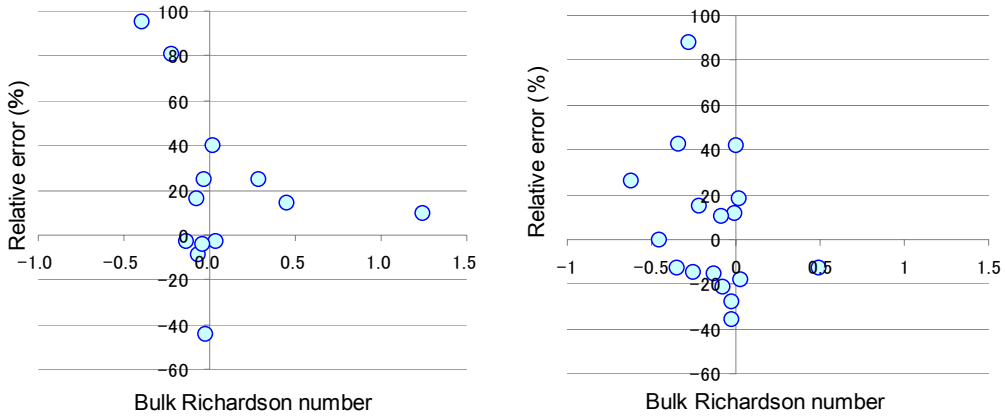

Fig.7 Relation between Bulk Richardson Number and relative errors (%) of SAR wind speeds for 300m-averaging at Hiratsuka (left) and 200m-averaging at Shirahama (right), respectively.

6. Conclusions

SAR wind speeds retrieved from 61 ENVISAT/ASAR images are validated in the inshore areas, Hiratsuka and Shirahama, Japan. Firstly, the relation between pixel-averaging size and accuracy of SAR-retrieved wind speed is examined. As a result, in Hiratsuka, the minimum RMSE of 2.30 m/s is achieved when 300m-averaging is applied, while that of 1.93 m/s is obtained in Shirahama when 200m-averaging is applied. These accuracies are lower than those reported for open oceans in previous studies. It also is shown that strong backscatters from the observation tower itself greatly affect the accuracy when the pixel-averaging size is less than 200m. Then, in order to remove the effect of the tower, the center of the averaging area is moved toward 500m offshore. As a result, in this case, a smaller averaging area is found to result in more accurate wind retrieval for Hiratsuka, compared to the case including effects from the observation tower. On the other hand, for Shirahama, a larger averaging area is found to be more suitable than in case including the tower. This difference of the suitable averaging area is caused by effects of speckle noise. In case with small effects of speckle noises, pixel averaging for a smaller area leads to more accurate wind retrieval, while a larger-area averaging is more effective for images with large effects of speckle noises. From the comparison between fetch and error of SAR wind speed, the effect of the fetch on the relative error of SAR wind speeds is not clearly detected in this study. On the other hand, it is shown that SAR wind speeds depends on atmospheric stability and tend to be overestimated under the unstable atmospheric condition. To reduce this kind of error, it is desirable to use a model function taking “Equivalent Neutral Wind” into account.

Acknowledgments

Envisat/ASAR scenes were acquired from the European Space Agency under the cooperative research project “Offshore wind resource assessments using SAR and MM5 over Japanese coastal waters”, C1P4068. The data observed in Hiratsuka was provided by National Research Institute for Earth Science and Disaster Prevention (NIED) and Institute of Industrial Science, the University of Tokyo (IIS) through influence of Mr. Isao Watabe. The data observed in Shirahama was provided by Disaster Prevention Research Institute Kyoto University (DPRI). This study is supported by a Grant-in-Aid for Scientific Research (B)(2) 19360406 and a Grant-in-Aid for Young Scientists (A) 19686052 from the Ministry of Education, Science, Sport and Culture, Japan.

Reference

1. Vachon, P.W, F. W. Dobson, Validation of wind vector retrieval from ERS-1 SAR image over the ocean. The Global Atmosphere and Ocean System 1996; 5: 117-187.
2. Goldfinger, A. Estimation of Spectra from Speckled Images**.** IEEE Transactions on Aerospace and Electronic Systems 1982; AES-18: 5: 675-681.
3. Horstmann J., S. Lehner, W. Kock, and R. Tonboe. Computation of wind vectors over the ocean using spaceborne synthetic aperture radar. John Hopkins APL. Tech. Dig 2000; 21(1):100–107.
4. Ad Stoffelen and David Anderson. Scatterometer data interpretation: Estimation and validation of the transfer function CMOD-4. Journal of Geophysical Research 1997; 102, C3:5767-5780.
5. Mouche, A. A., D. Hauser, J. Daloze, and C. Gueri. Dual-Polarization measurements at C-Band over the ocean: result from airborne radar observations and comparison with ENVISAT ASAR data. IEEE Transaction on Geoscience and Remote Sensing 2005; 43: 4: 753-769.
6. Charnock, H., “Wind stress on a water surface”, Quarterly Journal of the Royal Meteorological Society, 1955, Vol.81, pp.639-640.
7. Wu, J., Wind stress coefficients over sea surface near neutral conditions – A revisit”, 1980, Journal of Physical Oceanography, Vol.10, pp.727-740.
8. Gash, J. H. C., A note on estimating the effect of a limited fetch on micrometeorological evaporation measurements. Boundary-Layer Meteorology 1986; 35:4:409-413.
9. Smedman, A, U. Högström, H. Bergström, A. Rutgersson, K. K. Kahma and H. Pettersson. A case study of air-sea interaction during swell conditions. Journal of Geophysical Research 1999; 104: C11: 25833–25851.
10. Cressman, G. P.: An operational objective analysis system. 1959, Monthly Weather. Review, 87(10) pp:367-374.
11. Lehner, S., J. Hostmann, W.Koch and W. Rosenthal. Mesoscal wind measurements using recalibration ERS SAR images. Journal of Geophysical Research 1998; 103: C3: 7847-7856.
12. Liu, W. Timothy, Wenqing Tang. Equivalent neutral Wind. JPL publication 1997; 96-17.